Fluorination of MnO_2 Nanostructures for Lithium-Ion Energy Storage

Geoffrey Xiao, Mahidi Hassan, Sam Kulesa

MATE 492: Senior Design Project II

Submitted March 19, 2018

Abstract:

Lithium-ion batteries are becoming increasingly more important in satisfying the world's energy demands. The significant progress made in the decades since its conception has slowed, and present materials are reaching their limit in performance and cost. Manganese oxides offer an alternative which is less expensive and offers better performance, but suffer from low long-term stability. This project investigates different methods of fluorinating α-MnO_2 to improve electrochemical cycling performance. We report the first-ever synthesis of fluorinated α-MnO_2 through three different methods.

Background and Problem Statement

2017 saw the announcement or completion of large-scale solar energy projects in all but five states in the US [1], with similar or higher growth around the world. Demand also grew for consumer electronics, electric cars, and aerospace vehicles. There is no doubt that 2018 and the decades to come will bring an even higher demand for such devices, and along with it, increasing needs for energy storage.

The leading technology for energy storage in many applications is lithium-ion battery technology. As with any battery, a charged lithium-ion battery consists of an electron-rich anode and an electron deficient cathode, shown in Figure 1. When the two are connected, electrons flow from the anode to the cathode, generating a current which can power a device. Lithium-ions move between the electrodes through the electrolyte, which is an electrical insulator but allows ion flow.

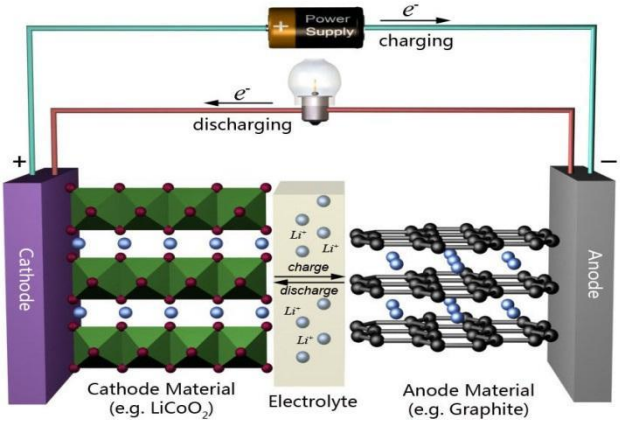

Figure 1. Conventional Li-ion battery. Adapted from School of Chemical Sciences, University of Illinois. http://www.scs.illinois.edu/murphy/Ran/research/energystorage.htm

Today's lithium-ion batteries typically use layered materials; two of the most popular electrode materials are graphite for the anode and $LiCoO_2$ for the cathode, as these layered materials intercalate lithium-ions well.

While there are many different issues, $LiCoO_2$ has two specific issues: limited capacity, and cost. Cobalt is not a common material in the earth's crust and is only abundant in a few areas of the world, many of which are politically volatile. This limits the supply of cobalt, making it more expensive and unreliable. Also, while $LiCoO_2$ has a theoretical capacity of 273 mAh/g, progress in increasing the experimental capacity has slowed around 180 mAh/g. Similar economic or performance issues also exist for other common cathode materials, including $LiFePO_4$ and $LiNi_{0.8}Co_{0.15}Al_{0.05}O_2$ [2]. Reducing the cost and increasing the performance of lithium-ion batteries will require not only new processing techniques, but also new materials.

Manganese is a material that is estimated to be at least 100 times more abundant than cobalt in Earth's crust and with a diverse set of possible supply chains [3]. There has been recent interest in the "tunnel-structured" α-MnO_2, seen in Figure 2a [4], which has a high theoretical

specific capacity of 304 mAh/g and experimental capacities near 255 mAh/g [5]. α-MnO_2 has also been given consideration as a cathode in "beyond-lithium" energy storage, like Mg-ion batteries [6]. There is one disadvantage to α-MnO_2: its low capacity retention. The aim of this project is to improve the capacity retention using fluorination.

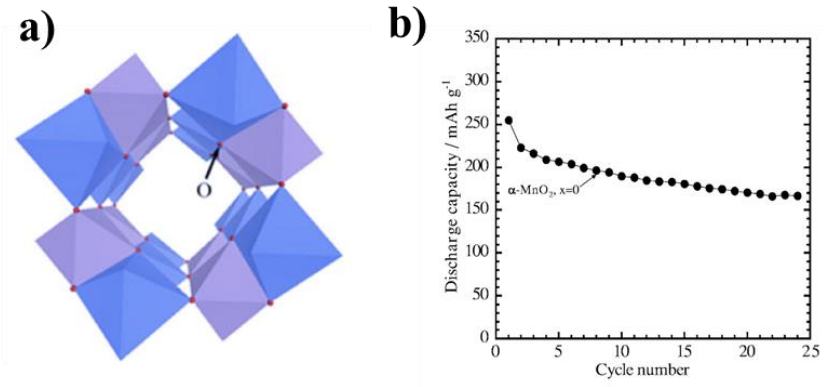

Figure 2. a) Tunnel structure of a-MnO_2. Adapted from [4]. **b)** Cycling data of a-MnO2, from Sasaki et al [5].

Rationale

Low capacity retention, or cyclability, means that after a low number of cycles, there is a significant decrease in the capacity. While virtually all cathode materials lose capacity over time, α-MnO_2 is especially poor in this regard, with 65-70% retention over 25 cycles as seen in Figure 2b [4]. For use in an application like a cellphone which requires thousands of cycles, such a low capacity retention is not sufficient.

The low cyclability of α-MnO_2 is not fully understood, but it is theorized to be due to instability from the repeated insertion of lithium-ions during cycling, and the dissociation of Mn^{2+} from the lattice. It is thought that phase changes may occur from these two, in addition to general destabilization of the tunnel-like α-MnO_2 structure. To resolve this issue in similar metal oxides, fluorination has been executed and has seen great results (Figure 3). By incorporating fluorine at oxygen sites (and thus generating stronger Mn-F bonds where there were weaker Mn-O bonds), the stability can be enhanced, providing a better capacity retention. This has been seen in $LiNiCoMnO_2$, $LiTi_2O_4$, and other metal oxides with positive changes to cyclability occurring even with relatively low fluorine additions [7] [8]. Cation exchange has also been researched extensively for metal oxide cathodes, but anion exchanges (like fluorination) have not been as well-studied.

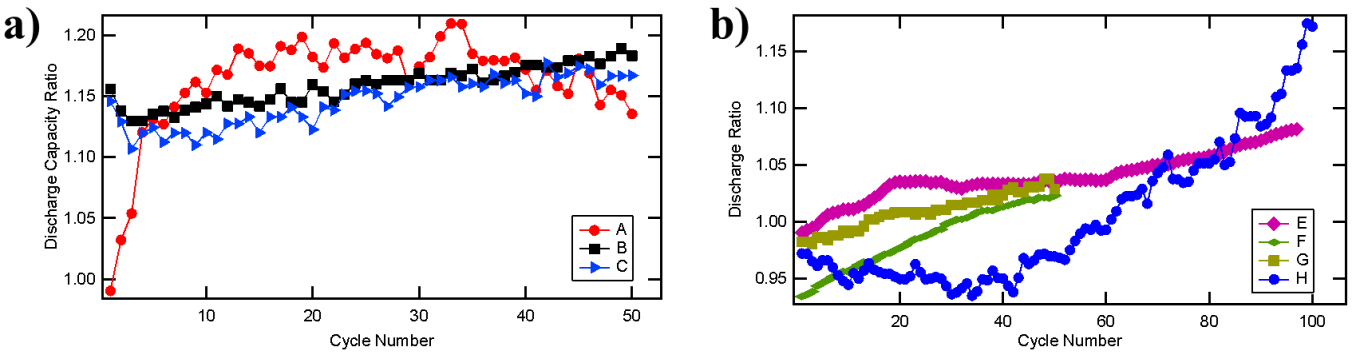

Figure 3. Discharge ratio is defined as the discharge capacity of the fluorinated material divided by the discharge capacity of the un-fluorinated material. A-C **(a)** are LiM_2O_4 spinel type and E-H **(b)** are layered $LiMO_2$ type materials[1].

Objective

Previous testing of α-MnO_2 saw capacity retentions around 65% after 25 cycles, as seen in Figure 3. Our goal is to improve the capacity retention while having minimal negative impact on the initial discharge capacity. Setting a goal number for the initial discharge capacity is tough with many free variables such as anode material, electrolyte choice, and operating voltage, but as long the fluorinated α-MnO_2 maintains a higher capacity versus a pristine α-MnO_2, the project would be considered successful. Reaching a capacity retention of 75% at 25 cycles or 60% at 100 cycles would be considered a significant accomplishment.

Experimental Approach

Synthesis and Fluorination

Synthesis of α-MnO_2 nanowires is performed using a high-pressure, hydrothermal method [9]. 1 mmol $KMnO_4$ and 1 mmol of NH_4Cl were dissolved in 20 mL of de-ionized water. A 25 mL Teflon-lined autoclave was then filled with the solution and heated to 150°C for 24 hours. The powder product was then filtered, rinsed, and grinded, and then dried at 100°C for several hours to remove excess water. The synthesized product is K_xMnO_2, with x ~ 0.13%. The K+ ions are confined within the tunnels to stabilize the crystal structure.

[1] A is $LiMn_2O_4$ / $LiMn_2O_{3.98}F_{0.08}$, B is $LiMn_{1.8}Li_{0.2}O_4$ / $LiMn_{1.8}Li_{0.2}O_{3.88}F_{0.12}$, C is $Li[Mn_{1.8}Li_{0.1}Ni_{0.1}]O_4$ / $Li[Mn_{1.8}Li_{0.1}Ni_{0.1}]O_{3.9}F_{0.1}$ [8]. E is $LiNi_{0.5}Mn_{1.5}O_4$ / $LiMn_{1.5}Ni_{0.5}O_4$ / $LiMn_{1.5}Ni_{0.5}O_{3.9}F_{0.1}$ [23]. F is $Li[Ni_{1/3}Co_{1/3}Mn_{1/3}]O_2$ / $Li[Ni_{1/3}Co_{1/3}Mn_{1/3}]O_{1.95}F_{0.05}$ [24]. G is $Li[Ni_{0.6}Co_{0.2}Mn_{0.2}]O_2$ / $Li[Ni_{0.6}Co_{0.2}Mn_{0.2}]O_{1.98}F_{0.02}$ [25]. H is $Li[Ni_{0.8}Co_{0.1}Mn_{0.1}]O_2$ / $Li[Ni_{0.8}Co_{0.1}Mn_{0.1}]O_{1.98}F_{0.02}$ [26].

To carry out the fluorination process, a vapor transport method was used [9], [10]. A schematic of this method can be seen in Figure 4. Essentially, α-MnO_2 and a fluorine source, polytetrafluoroethylene (PTFE) or polyvinylidene fluoride (PVDF), are placed in a ceramic boat inside of a glass tube which is heated to various temperatures and time durations using a ThermoFisher Lindberg Blue M Furnace. Argon gas is flown through the tube to carry the fluorine to react with the α-MnO_2. Importantly, in this method, the α-MnO_2 and fluoropolymer are physically separated by an aluminum barrier.

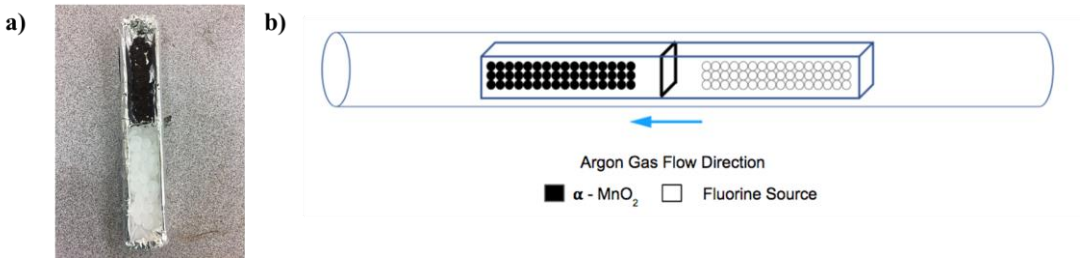

Figure 4. Schematic of the vapor transport method with barrier.

During the Fall Term, most of the fluorination attempts were dedicated to varying parameters such a fluorination time and temperatures to determine the optimal values. In Winter Term, modifications were made to the vapor transport process, and two new processes were also tried. One method that was employed was acid-leaching.

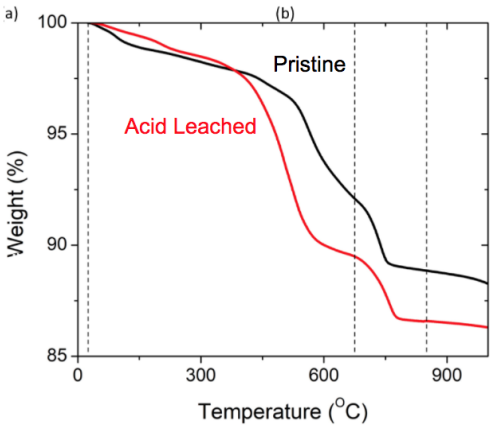

Figure 5. TGA data for pristine and acid-leached a-MnO_2, courtesy of Patrick West [12].

Synthesis of acid-leached MnO_2 is performed by combining 100 mg of pristine MnO_2 with 300 mL of 16 M nitric acid solution. The sample is kept in solution for 24, 48, or 72 hours before drying. During the acid leaching process, cation exchange between H^+ and K^+ ions and disproportionation of Mn ions occurs [22]. Together these two mechanisms introduce oxygen vacancies in the material, potentially enabling higher degrees of fluorine incorporation, as reported in thin-films fluorination studies [11].

TGA data for pristine and acid-leached samples is provided in Figure 4 [12]. As acid-leached material is more sensitive than pristine, lower temperatures were used for the acid-

leached α-MnO_2. The fluorinations in Fall Term ranged from 180-380 ^oC, and initially 320^oC was used for acid-leached, but 250^oC was used, after phase decomposition occurred in some samples at 320^oC. All fluorination were run for roughly 24 hours, as Fall experiments determined that there was a kinetic aspect to the fluorination, with higher changes in lattice parameter seen in longer-fluorinated samples.

Vapor Transport Modifications: Homogenous Mixing

The original fluorination setup for the vapor transport method consisted of placing the α-MnO_2 and fluorine source side-by-side, separated by aluminum foil in a ceramic boat. This approach unfortunately was not successful with either the pristine or acid-leached samples; the fluorine from the polymer had not incorporated into the α-MnO_2. Because of this, different modifications were tested to create a setup which would lead to successful fluorination.

The first modification was to create a homogenous mix using the α-MnO_2 and the fluorine source. A schematic can be seen below in Figure 6. This modification was done using PVDF and PTFE. In the PVDF sample, the PVDF melted and combined with the α-MnO_2 to form an unknown solid. Typical PVDF solvents such as N-methyl-2-pyrrolidone and methanol were not able to dissolve the new compound, so it is likely PVDF decomposed into a new product. In the PTFE sample, the α-MnO_2 could be extracted from the PTFE by hand. A better extraction method would involve dissolving the PTFE in a solvent, but unfortunately few solvents are capable of dissolving PTFE due to its chemical stability.

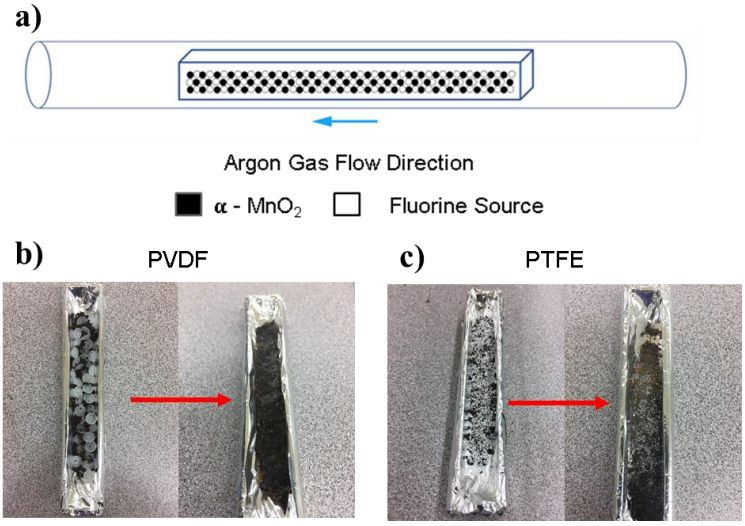

Figure 6. a) A schematic of the setup. **b)** PVDF melted and formed a new material, from which α-MnO_2 could not be extracted. **c)** The α-MnO_2 could be extracted from the PTFE mixed sample.

Vapor Transport Modifications: Intimate Contact

The next modification that was implemented consisted of placing the α-MnO_2 and the fluorine source in the ceramic boat, side-by-side, without a barrier between them. A schematic for this modification can be seen below in Figure 7. After fluorination the materials had touched each other, but towards one end of the ceramic boat, there was α-MnO_2 that was extractable which could be removed for analysis.

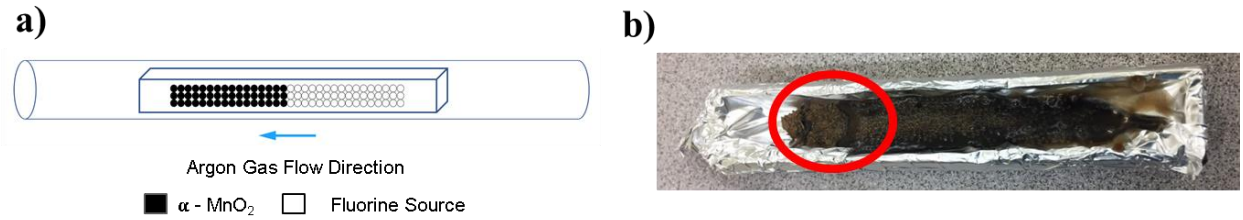

Figure 7. a) Schematic of the setup. **b)** α-MnO_2 (red outline) could be extracted.

Vapor Transport Modifications: Filter

This modification consisted of creating a layered setup—the fluorine source and MnO_2 were stacked on top of each other, but separated with a strip of aluminum foil with holes. The purpose of this 'filter' was to maximize vapor transport between the α-MnO_2 and PVDF, but to minimize physical contact between the α-MnO_2 and PVDF. A schematic for this modification can be seen below in Figure 8.

Figure 8. a) Schematic of the modification. **b)** From left to right, the aluminum filter; the α-MnO_2 placed on top of the filter; and the α-MnO_2 after the fluorination process.

Solution Treatment Method

This method was originally developed by [13]. In this method, 50 mg of α-MnO_2 was mixed with various concentrations ($2.5*10^{-5}$ M and $2.5*10^{-2}$ M) of NH_4PF_6 in 100 mL of methanol. The powder-solution mixture was stirred for 20 hours. After the solution treatment, the α-MnO_2 was filtered and washed with water, and subsequently to 300^oC for 4 hours

Characterization

Along with each experimental approach, three techniques have been used for characterization. X-ray diffraction (XRD) is conducted on all samples using a Rigaku Miniflex provided by the Drexel Centralized Research Facility (CRF). As the crystal structure of α-MnO_2 is integral to its electrochemical performance, each attempt at fluoriantion is checked with XRD to verify the tunnel structure is still maintained. XRD is also useful for showing contaminants: for example, a procedure using PVDF may leave some PVDF coated on or mixed into the α-MnO_2. XRD can pick up extra peaks which may correspond to these contaminants.

Scanning electron microscopy (SEM) and energy-dispersive x-ray spectroscopy (EDX) were also conducted on a Zeiss Supra 50VP through the CRF. SEM is useful qualitatevly, to confirm the nanowire morphology of samples. While EDX is a powerful compositional technique, the fluorine and manganese peaks obstruct each other, and it is difficult to deconvolute the signals to show presence of fluorine. Instead, x-ray photoelectron spectroscopy (XPS) is conducted with a Physical Electronics VersaProbe 5000, which can show not only the presence of elements, but also bonding. For the previous example of sample contamination with PVDF, the XPS can distinguish between C-F bonds and Mn-F bonds, as the binding energies for these are different. In XPS, the fluorine 1s peak (~685 eV) should not overlap with the manganese (~641 eV) or oxygen peaks (~530 eV) [21].

Additional ASTM standards will be consulted throughout the project. Due to the need for XPS chemical composition analysis, ASTM E995 *Standard Guide for Background Subtraction Techniques in Auger Electron Spectroscopy and X-Ray Photoelectron Spectroscopy* will be used. In brief, the standard provides invaluable information for the appropriate methods of analyzing XPS data and extracting quantitative information on chemical composition. Another useful ASTM standard is ASTM E1523-15 *Standard Guide to Charge Control and Charge Referencing Techniques in X-Ray Photoelectron Spectroscopy*. During XPS, the sample may charge due to

repeated ejection of electrons, potentially shifting XPS peaks. The ASTM E1523-15 standard describes how XPS data can be charge corrected by referencing the 284.8 eV C1s peak due to C-C bonding. Due to the ubiquity of carbon, this C-C bond is present in all samples.

At this point electrochemical testing has not been performed. But in the Spring Term, electrochemical testing will be used to test the performance of fluorinated α-MnO_2. Primarily, charge-discharge cycles will be run with lithium anodes and liquid electrolytes, as per industry best-practices or standards from SAE International such as J-3159 *Techniques for measuring the properties of lithium and lithium-ion battery anode active materials* or J-3021-201410 *Recommended Practice for Determining Material Properties of Li-Battery Cathode Active Materials* to find the initial capacity and cyclability. Further electrochemical testing will include rate capability tests, which contribute to maximum charging speeds, and cyclic voltammetry, which tests reversibility and stability.

Results and Discussion

Characterization of Pristine α-MnO_2

First, the synthesis of un-fluorinated, pristine nanowire α-MnO_2 is confirmed. The nanowire morphology is desirable due to its high surface area for lithium ion intercalation and low dimensionality enabling un-impeded lithium ion diffusion [14]. The nanowire morphology is confirmed using a scanning electron microscopy (SEM) (Figure 9a). Powder x-ray diffraction (XRD) patterns were also obtained with a Rigaku SmartLab using the Cu kα_1 and kα_2 lines. The XRD patterns were indexed according to a I4/m space group and lattice parameters were found using the WinCSD software. The XRD patterns (Figure 9b) likewise confirms the crystalline structure (PDF#01-077-1796) and the absence of second phases.

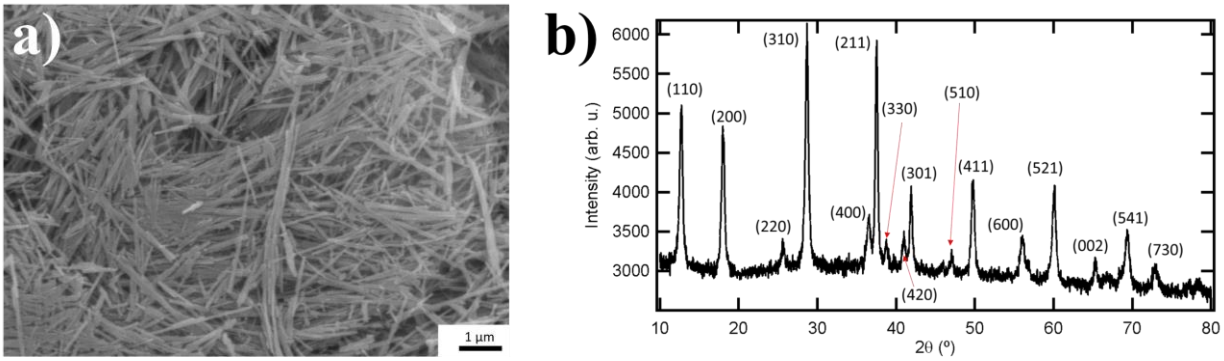

Figure 9. a) SEM confirms the nanowire morphology. **b)** XRD confirms the tetragonal I4/m crystalline structure of pristine α-MnO_2. No secondary phases are detected.

Conventional Vapor Transport Method

During the Fall quarter, the conventional vapor transport method was performed at 180°C, 280°C, and 380°C for 4, 12, and 24 hours using PTFE as the fluorine source. While the XRD pattern (Figure 10) of the 24 hour, 380°C fluorinated sample shows structural preservation, the XPS spectra provides no evidence of fluorination (the fluorine peak should be around 690-685 eV [15]). Previous work has shown that greater fluorine incorporation occurs when the vapor transport process is performed at high temperatures and for long time durations [16]. Therefore, it is unlikely any of the samples from Fall Term were fluorinated successfully.

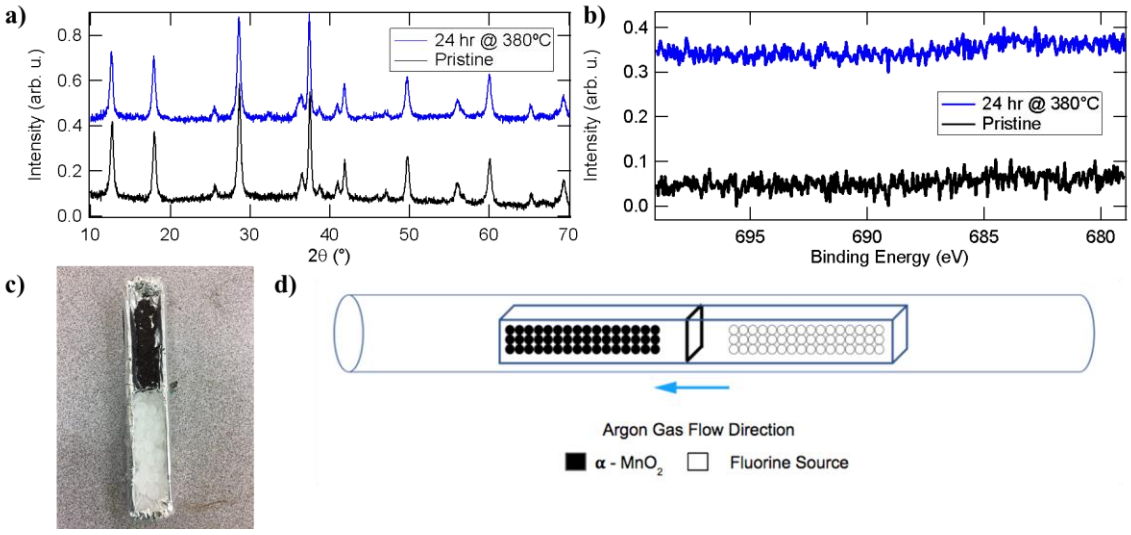

Figure 10. a) XRD pattern of the fluorinated and pristine α-MnO_2. **b)** XPS spectra of the fluorinated and pristine α-MnO_2. Fluorine peaks around 685-690 eV are absent. **c)** and **d)** Schematic of the conventional vapor transport method.

Conventional Vapor Transport Method using Acid-Leached α-MnO_2

It has been shown that oxygen vacancies allow for increased incorporation of more fluorine [17]. As discussed earlier, α-MnO_2 treated with nitric acid contains oxygen vacancies. When acid-leached α-MnO_2 is fluorinated with the conventional vapor transport method at 200°C and 250°C for 24 hours and with PTFE as the fluorine source, the XRD pattern confirms preservation of the tunnel-like structures, but the XPS spectra show that fluorine is absent (Figure 11).

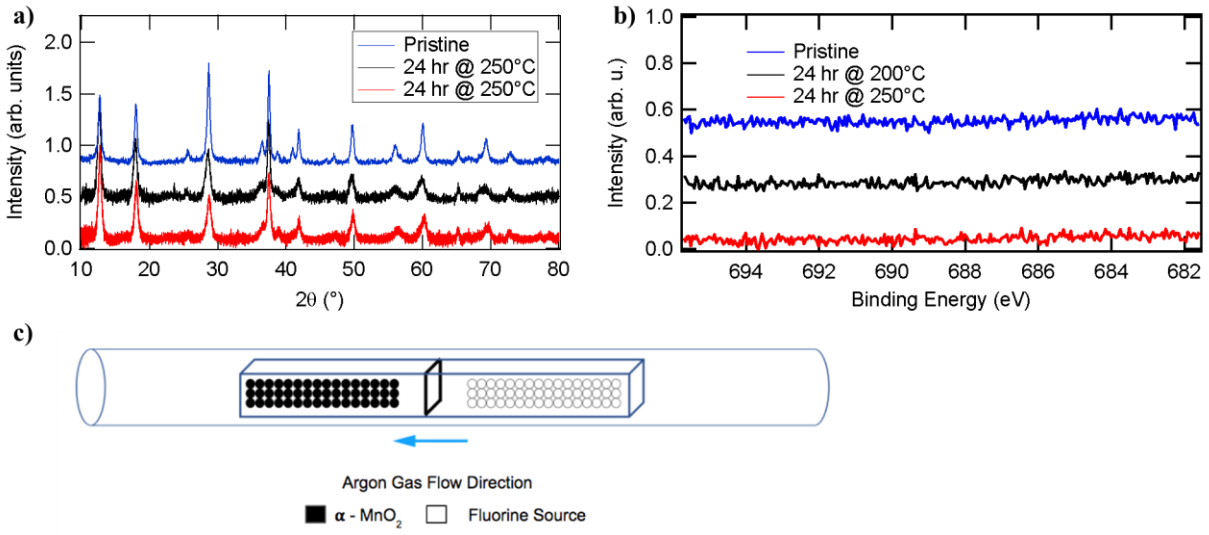

Figure 11. a) XRD showing structural preservation at 250°C. **b)** XPS shows no preceense of fluorine in samples and **c)** original vapor transport method used for acid-leached MnO_2.

Intimate Contact Fluorination Methods

PTFE was homogenously mixed with α-MnO_2 and the resulting mixture was heated to 380°C for 24 hours ("PTFE Mixed"). The little remaining α-MnO_2 powder was extracted from the homogenous mixture by hand. PVDF was placed in close contact with α-MnO_2, and was heated to 250°C for 40 hours ("PVDF Mixed: No Barrier"). While there was contact between the α-MnO_2 powder and the melted PVDF, most of the α-MnO_2 did not touch the PVDF and could be readily extracted by hand.

The XRD pattern of the "PVDF Mixed" sample (Figure 12a) shows that the α-MnO_2 peaks are all preserved, indicating that the fluorination process preserved the tunnel structures. There are, however, several new peaks (Green arrows, Figure 12a). It is not immediately clear what structure or material these new peaks correspond to. The distinct peaks characteristic of PVDF (Figure 13a) are not readily indexed. Perhaps a fluoride such as KF or MnF_2 formed or the α-MnO_2 decomposed into MnO, Mn_3O_4, or Mn_2O_3. Several of the possible decomposition and product reaction peaks align, but a clear determination of the origin of the new peaks is difficult. Meanwhile, the XRD of the "PTFE Mixed" sample (Figure 12) shows that the α-MnO_2 structure is not preserved. The large ~18° peak in the "PTFE Mixed" sample may be due to PTFE. Several of the XRD peaks in the "PTFE Mixed" sample also match with the new peaks seen in the "PVDF Mixed" sample suggesting that the two decomposed or reacted into similar products.

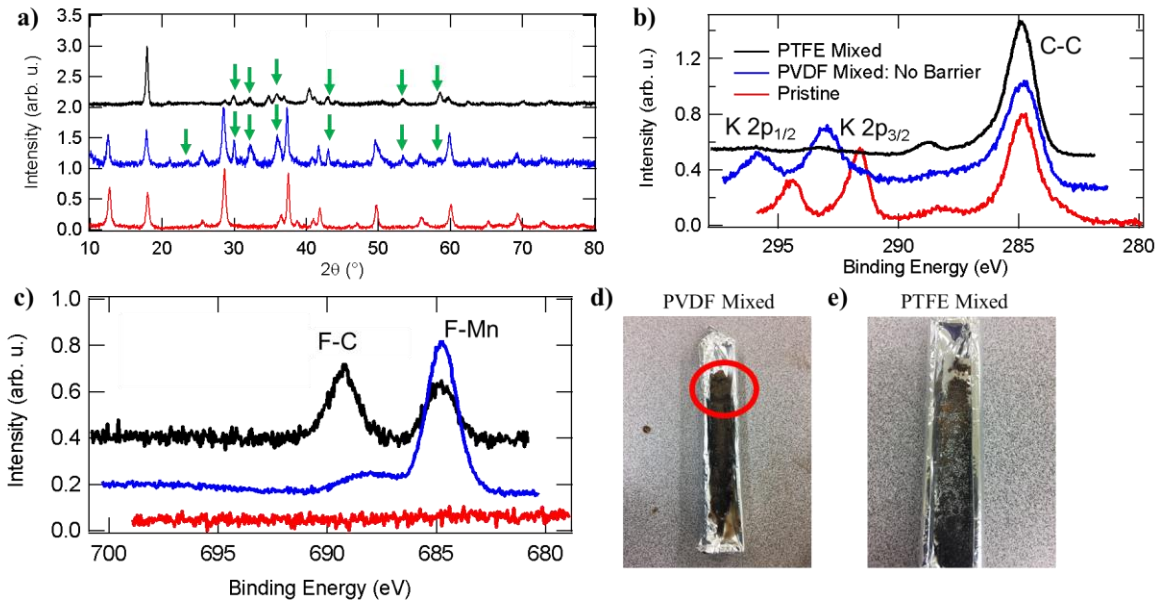

Figure 12. a) XRD patterns of the samples. Green arrows highlight new, unknown peaks. **b)** XPS in C and K regions. **c)** XPS in F region. **d)** Picture of the "PVDF Mixed" sample. The red outline highlights the extractable α-MnO_2. **e)** Picture of the "PTFE Mixed" sample.

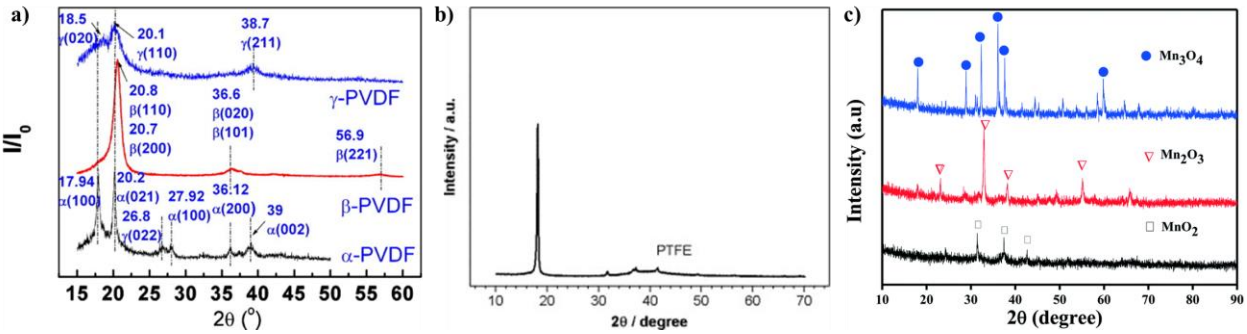

Figure 13. XRD patterns of **a)** PVDF [18], **b)** PTFE [19], and **c)** forms of Mn_xO_y [20].

The XPS spectra (Figure 12) of the "PVDF Mixed" and "PTFE Mixed" show fluorine peaks. The presence of two fluorine peaks can be attributed to a F-C and a F-Mn bond [15]. The F-Mn bond is indicative of fluorine incorporation into the α-MnO_2 and the F-C bond is directly due to F-C bonds from the polymer fluorine source. The relative ratio of the F-Mn to F-C bond in the "PTFE Mixed" sample is due to the intimate contact between the PTFE and α-MnO_2 in the "PTFE Mixed" sample. That the "PVDF Mixed" sample has a larger relative F-Mn peak to F-C peak ratio is due to fact that the α-MnO_2 was not as intimately contacted with the polymer in the "PVDF Mixed" sample. Similarly, the C-C peak is much larger than the K2p peak in the "PTFE Mixed" sample (Figure 12b), again suggesting that a large amount of polymer residue remains in the "PTFE Mixed" sample. The "PTFE Mixed" and "PVDF Mixed" K2p peaks are also

significantly shifted with respect to the pristine K2p peaks. The K2p peak can shift due to different bondings (e.g. K-Cl vs K-F), but such shifts are less than 1 eV [21].

Ultimately these results have shown that fluorination of α-MnO_2 is possible. Increasing the contact between the fluorine source and α-MnO_2 allows for fluorination but leads to polymer contamination and structural degradation.

Filter Method

In this method, the vapor contact between the fluorine source and the α-MnO_2 was maximized, but the fluoropolymer was not in contact with the α-MnO_2 ("Filter" sample). This "Filter" sample was fluorinated with PVDF at 280°C for 24 hours. A 48 hour acid-leached α-MnO_2 was used for the fluorination process. The XRD pattern shows that the structure is preserved, with the exception of one new XRD peak ~32° (Figure 14a). A similar ~32° peak appeared in the samples from the previous *Intimate Contact* section. Further, the K2p peaks of the "Filter" sample are not shifted with respect to the K2p peaks of the "Pristine" sample, and there is no F-C bond in the "Filter" sample. These results are extremely encouraging as they show that the presence of fluorine, the absence of the fluoropolymer, and the preservation of the α-MnO_2 crystal structure in the fluorinated sample.

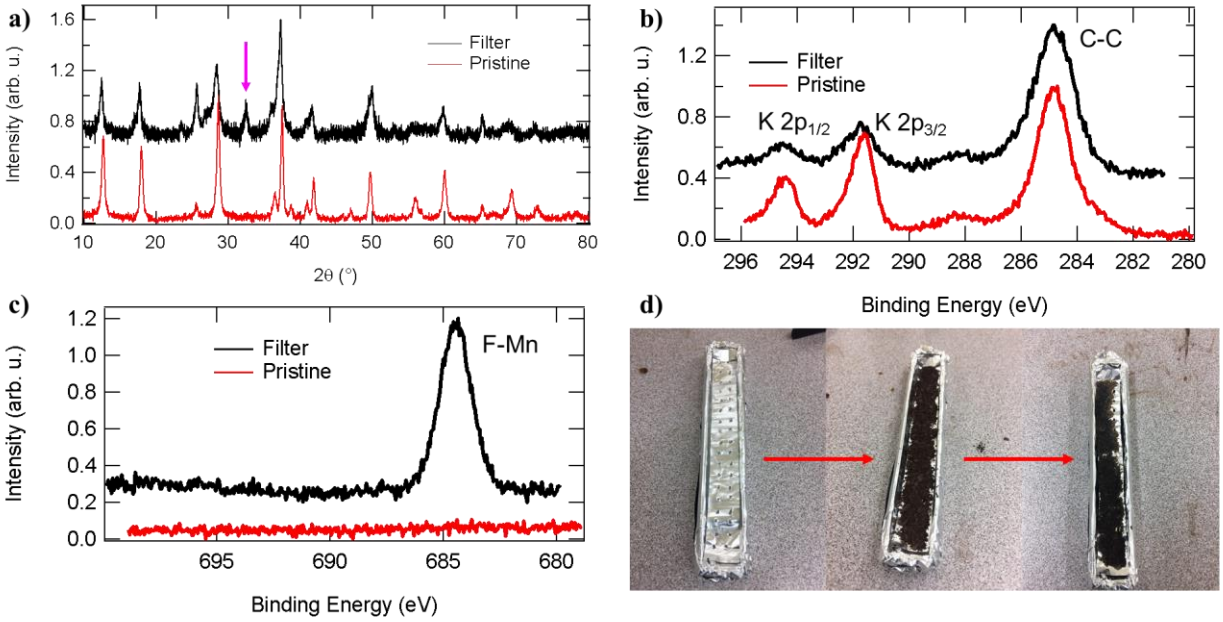

Figure 14. a) XRD for filter method. **b)** XPS in C and K regions. **c)** XPS in F region shows F-Mn and no F-C. **d)** From left to right, the aluminum filter; the α-MnO_2 placed on top of the filter; and the α-MnO_2 after the fluorination process.

Low Temperature Solution Treatment

In this method, 50 mg of α-MnO_2 was mixed with various concentrations ($2.5*10^{-5}$ M and $2.5*10^{-2}$ M) of NH_4PF_6 in 100 mL of methanol. The powder-solution mixture was stirred for 20 hours. After the solution treatment, the α-MnO_2 was filtered and washed with water, and subsequently to 300°C for 4 hours. In the XRD patterns (Figure 15b), not only is the structure of the solution-treated samples the same as the pristine α-MnO_2, but also there are no new, unknown peaks, as was the case in the vapor transport methods. This suggests that the new XRD peaks seen in the vapor transport methods may be due to heat-induced degradation of the α-MnO_2 rather than due to the formation of new fluorine-containing compounds such as KF or MnF_2. Both the vapor transport samples and the solution-treated samples have fluorine, but the vapor transport methods were treated at higher temperatures for significantly longer time lengths than the solution-treated samples.

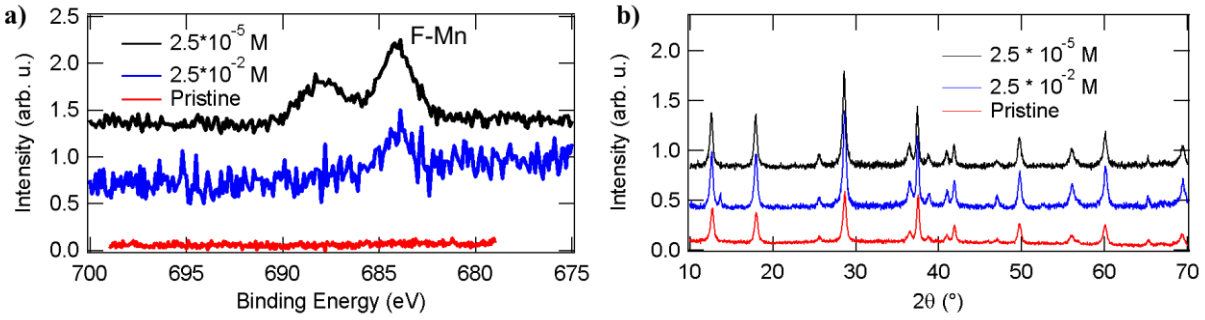

Figure 15. a) XPS in the F region confirms the presence of fluorine. **b)** XRD patterns of the samples shows structural preservation.

The XPS spectra of the solution-treated samples also confirms the presence of fluorine. The XPS data, however, is unintuitive in that the lower concentration sample ($2.5*10^{-5}$ M) actually appears to have a sharper and more well-defined fluorine peak suggesting it has more fluorine than the $2.5*10^{-2}$ M sample. Because 50 mg of α-MnO_2 and 100 mL of solution were used, $2.5*10^{-5}$ M translates to $2.5*10^{-6}$ mol of NH_4PF_6 and $5.7*10^{-4}$ mol of MnO_2. Considering that NH_4PF_6 has 6 potential flourine sources, it is not entirely unreasonable that the $2.5*10^{-5}$ M sample has such strong F-Mn peaks. The presence of two fluorine peaks in the $2.5*10^{-5}$ M sample is more puzzling. Previously, the two flourine peaks could be attributed to F-C and F-Mn bonds. Here, there is no fluoropolymer, and neither nitrogen nor phosphorous were detected in the XPS spectra. The F-Mn XPS peak could shift depending on the oxidation state of Mn (Mn^{4+}

vs. Mn^{3+} vs. Mn^{2+}), but these shifts are smaller than 1 eV [21]. It is unclear what causes the two fluorine peaks, and more characterization needs to be performed.

Discussion

Overall, these results show that the conventional vapor transport method, while previously successful for thin films, is unable to successfully fluorinate α-MnO_2. To this end, several modifications to the vapor transport method were developed. These modifications show that successful fluorination requires maximizing the vapor contact between the α-MnO_2 and the fluoropolymer source. Actual contact between the fluoropolymer and the α-MnO_2, however, leads to polymer contamination and possible structural degradation. Further, a new solution treatment method has been able to achieve topotactic fluorination.

Throughout these experiments, there are many parameters to tune: acid-leached α-MnO_2 for increased oxygen vacancies versus pristine α-MnO_2; the fluorination method (vapor transport, modified vapor transport, and solution method); the time and temperature of heat treatment; and the fluorine source (PTFE vs. PVDF in the vapor transport method; the fluorine salt—NH_4PF_6, $(NH_4)_3AlF_6$, NH_4BF_4, and NaF in the solution method). Thus far it has been shown that topotatacitc flourination of α-MnO_2 is possible. In future work, a systematic study of the various fluorination parameters will be performed.

Timeline and Upcoming Tasks

For the Fall and Winter Terms, most of the lab time was dedicated to fluorinating pristine and acid-leached α-MnO_2 using various methods and modifications in order to achieve successful incorporation of fluorine into the α-MnO_2 material. For the Spring Term, the fluorination process needs to be perfected for the aluminum filter method as well as the solution method. For both processes, multiple fluorinations need to be conducted with the same parameters in order to ensure that the process is consistent and repeatable.

Additionally, after the fluorinations have been conducted, electrochemical testing will be done to determine if the new α-MnO_2 material has improved energy density as well as capacity retention. In addition to electrochemical characterization, more structural characterization will be done, such as XRD to track changes in crystal structure and lattice parameters of the material

upon battery cycling. Finally, magnetic characterization will also be done to assess magnetic properties. An updated Gantt chart can be seen below in Figure 16.

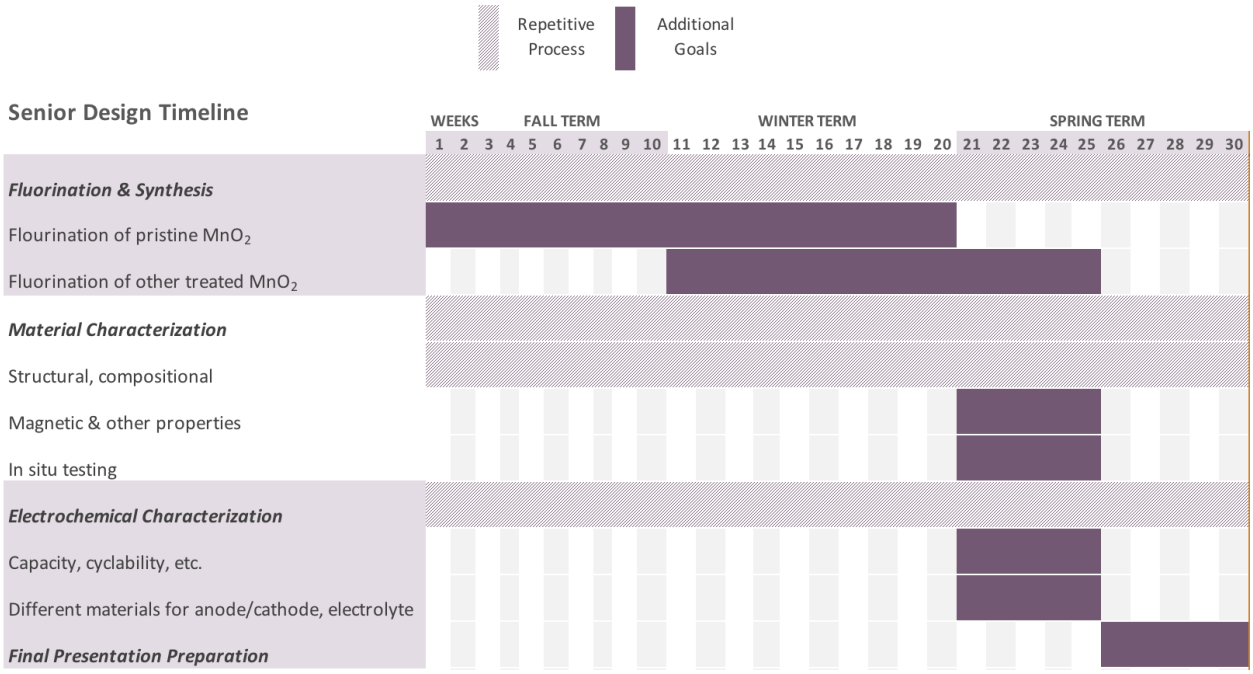

Figure 16. Gantt chart and timeline for project. Gray represent processes which will be repeated through process, purple represents tasks with a more fixed time range

Constraints

The main constraint during Fall and Winter Terms was conducting fluorinations due to limited availability of a fume hood and tube furnace. However, with the addition of a new tube furnace in the lab, fluorination experiments were able to be conducted significantly faster; approximately 5-6 experiments were carried out each week. Additionally, limited availability of XRD and XPS equipment are still minor constraints, but this issue was alleviated by proper communication with staff and excellent time management.

Economically, the raw materials being used are relatively cheap but the characterization equipment used such as XRD and XPS have expensive costs associated with using them. However, the project is being generously funded by Dr. May's Oxide Films and Interfaces (OFI) group and Dr. Pomerantseva's Materials Electrochemistry Group (MEG). The main constraint of Winter Term was modifying the vapor transport method in order to achieve successful fluorination; besides that, this project does not pose any societal, ethical, or political issues.

Table 1. Main safety concerns and associated safety measures.

Constraint	Description
Economic	Raw materials are relatively cheap Characterization tools are expensive
Societal, Ethical, Political	None
Legal	None
Time	Fluorinations take 24 hours, battery cycling takes days
Health & Safety	Some safety hazards in synthesis
Manufacturability	Significant development required before mass production feasible
Environmental, Sustainability	None

Safety

Caution needs to be exercised when working in the laboratory at all times. Synthesis and fluorination of MnO_2 requires the use of high pressure autoclaves and high temperature settings in the tube furnace. All standard operating procedures (SOPs) were followed while working in the lab. Personal protection equipment (PPE) such as gloves and safety glasses were utilized to ensure materials were not contaminated as well as to protect all persons in the lab from chemical spills and injury.

Table 2. Main safety concerns and associated safety measures.

Major process	Sub process	Safety concerns	Safety Measures
Synthesis	Hydrothermal reaction	High pressure reaction	Autoclaves designed with gas release valves
	Chemicals	16 M nitric acid, Hydrogen peroxide	Two layers of nitrile gloves
Fluorination	Fluorine-containing materials (PVDF, PTFE)	Toxicity, Reactivity	Fume Hood, extra hours of flow
	Temperatures up to 400 ^oC	High temperatures	Fume hood, insulated gloves, furnace insulation
	Compressed gas cylinders (N_2, Ar, Air)	Compressed Gas	Pressure lock and wall-chain systems
Material Characterization	XRD	X-ray radiation	Sealed shielding door, fail-safe lock
Electrochemical testing	Assembling coin cell	Explosive reaction of lithium with water	Glovebox with controlled humidity
	Electrochemical cycling	Electrical Dangers	Grounded equipment, Warning signs around live circuits
	Lithium-ion Batteries	Short circuiting batteries leading to explosions	Temperature monitoring, Limit charging rates and charging times

Budget

A budget for the project is provided in Table 3. This project is supported by the Materials Electrochemistry Group (PI: Dr. Ekaterina Pomerantseva) and the Oxide Films & Interfaces Group (PI: Dr. Steven May) at Drexel University. The materials and equipment to be used for fluorination and testing are readily available through these labs and an XRD subscription has been provided to the group by Dr. May. Any additional expenses incurred are expected to be small and will be provided through the supporting research groups.

Table 3. Budget for the project, with a real cost column which considers resources which already exist in the MEG and OFI and did not need to be purchased for sole use in this project

	Item	Cost($)	Real Cost ($)	Provider
Lab Supplies	Sample capsules	20	0	OFI
	Quartz tube	50	0	OFI
	Aluminum Foil	10	0	OFI
	Acetone	30	0	OFI
	IPA	30	0	OFI
	Argon Gas	300	55	OFI
	Miscellaneous	20	0	OFI
	PTFE	50	50	OFI
	Subtotal:	***510***	***105***	
Lab Equipment	Tube Furnace	2000	0	OFI
	Autoclave	3000	0	MEG
	Subtotal:	***5000***	***0***	
Equipment Subscription	XRD (Rigaku SmartLab) (9 months)	1000	1000	OFI
	XPS (PHI VersaProbe 5000) (9 months)	3000	0	OFI
	SEM/EDS (Zeiss Supra 50VP, EDAX) (9 months)	2500	0	OFI
	Subtotal:	***6500***	***1000***	
Raw Materials	$KMnO_4$	50	0	MEG
	NH_4Cl	20	0	MEG
	De-ionized Water	30	0	MEG
	Miscellaneous	20	0	MEG
	Subtotal:	120	***0***	
Personnel	2 Salaried Materials Engineer, BS	136,000	0	
	Salaried Materials Engineer, BS/MS	72,000	0	
	2 Graduate Student Mentors	100,000	0	
	2 Project Advisors	50,000	0	
	Subtotal:	***358,000***	***0***	
	Total:	***$ 370,130.00***	***$ 1,105.00***	

Conclusion

Here, the details, from the scientific hypotheses to an in-depth overview of budgetary and time constraints, of the project have been thoroughly discussed. Such a review is critical not only

for team members to review the current progress and planned goals, but is also useful for graduate advisors and principal investigators to keep apprised of the work.

In this report, it was shown that α-MnO_2 has been successfully fluorinated using modified vapor transport methods and a solution treatment method. The XRD patterns show that the fluorination has preserved the tunnel structure of α-MnO_2 and the XPS data show that fluorine is indeed present in the material. These experimental results are, to the best of our knowledge, the first reported evidence of fluorinated α-MnO_2. The work done in the Winter quarter will set up the project for the Spring quarter, where the fluorinated α-MnO_2 will be electrochemically tested.

The experimental results also show that the vapor contact between the α-MnO_2 and the fluorine source is critical. In the conventional vapor transport method, the powder and fluoropolymer are separated by a barrier, thereby limiting contact between the two. In the modifications to the vapor transport and in the solution treatment method, the fluorine source has greater contact with the α-MnO_2. Yet while the contact between the fluorine source and α-MnO_2 needs to be maximized for fluorine incorporation, actual physical contact can lead to contamination. A fine balance must be satisfied to maximize fluorination and minimize contamination and structural degradation.

Acknowledgements

The senior design group would like to acknowledge advisors Dr. Steven May and Dr. Ekaterina Pomerantseva and thank both for their advice and efforts throughout the past terms. Mentors Bryan Byles and Jiayi Wang have also been helpful in providing instruction and advice on all aspects of this research project. The group would also like to thank the members of the Materials Electrochemistry Group, Oxide Films & Interfaces Group and Centralized Research Facility at Drexel University for their continued support.

References

[1] *Solar Energy Industries Association* https://www.seia.org/research-resources/major-solar-projects-list

[2] Nitta, Naoki, et al. "Li-ion battery materials: present and future." *Materials today* 18.5 (2015): 252-264.

[3] Gaines, Linda, and Paul Nelson. "Lithium-ion batteries: possible materials issues." *13th international battery materials recycling seminar and exhibit, Broward County Convention Center, Fort Lauderdale, Florida*. 2009.

[4] L.-T. Tseng et al., "Magnetic properties in α-MnO(2) doped with alkaline elements," Sci. Rep., vol. 5, p. 9094, Mar. 2015.

[5] Sasaki, Teruhito, et al. "Synthesis of Hollandite-Type $K_y(Mn_{1-x}M_x)O_2$ (M= Co, Fe) by Oxidation of Mn (II) Precursor and Preliminary Results on Electrode Characteristics in Rechargeable Lithium Batteries." *Electrochemical and Solid-State Letters* 8.9 (2005): A471-A475.

[6] Zhang, Ruigang, et al. "α-MnO_2 as a cathode material for rechargeable Mg batteries." *Electrochemistry Communications* 23 (2012): 110-113.

[7] Yue, Peng, et al. "A low temperature fluorine substitution on the electrochemical performance of layered $LiNi_{0.8}Co_{0.1}Mn_{0.1}O_{2-z}F_z$ cathode materials." *Electrochimica Acta* 92 (2013): 1-8.

[8] Choi, W., and A. Manthiram. "Superior capacity retention spinel oxyfluoride cathodes for lithium-ion batteries." *Electrochemical and solid-state letters* 9.5 (2006): A245-A248.

[9] Gao, Yongqian, et al. "A facile route to synthesize uniform single-crystalline α-MnO_2 nanowires." *Journal of crystal growth* 279.3-4 (2005): 415-419.

[10] Huang, Xingkang, et al. "Controllable synthesis of α-and β-MnO_2: cationic effect on hydrothermal crystallization." *Nanotechnology* 19.22 (2008): 225606.

[11] Katayama, T., et al. "Topotactic fluorination of strontium iron oxide thin films using polyvinylidene fluoride." *Journal of Materials Chemistry C* 2.27 (2014): 5350-5356.

[12] Data courtesy of Patrick West, Materials Electrochemistry Group.

[13] Kang, S-H., and M. M. Thackeray. "Stabilization of $xLi_2MnO_3 \cdot (1-x)\ LiMO_2$ electrode surfaces (M= Mn, Ni, Co) with mildly acidic, fluorinated solutions." *Journal of the electrochemical society* 155.4 (2008): A269-A275.

[14] Tompsett, David A., and M. Saiful Islam. "Electrochemistry of hollandite α-MnO_2: Li-ion and Na-ion insertion and Li_2O incorporation." *Chemistry of Materials* 25.12 (2013): 2515-2526.

[15] Nansé, G., et al. "Fluorination of carbon blacks: an X-ray photoelectron spectroscopy study: I. A literature review of XPS studies of fluorinated carbons. XPS investigation of some reference compounds." *Carbon* 35.2 (1997): 175-194.

[16] Onozuka, Tomoya, et al. "Reversible Changes in Resistance of Perovskite Nickelate $NdNiO_3$ Thin Films Induced by Fluorine Substitution." *ACS applied materials & interfaces* 9.12 (2017): 10882-10887

[17] Yoon, H. S., et al. "Properties of fluorine doped ZnO thin films deposited by magnetron sputtering." *Solar Energy Materials and Solar Cells* 92.11 (2008): 1366-1372.

[18] Li, Wenjing, et al. "Electric energy storage properties of poly (vinylidene fluoride)." *Applied Physics Letters* 96.19 (2010): 192905.

[19] Tian, Zhi Qun, et al. "Microwave-assisted synthesis of PTFE/C nanocomposite for polymer electrolyte fuel cells." *Electrochemistry communications* 8.7 (2006): 1158-1162.

[20] Nawaz, Faheem, et al. "The influence of the substituent on the phenol oxidation rate and reactive species in cubic MnO_2 catalytic ozonation." *Catalysis Science & Technology* 6.21 (2016): 7875-7884.

[21] NIST XPS Database: https://srdata.nist.gov/xps/ElmSpectralSrch.aspx?selEnergy=PE

[22] Hunter, James, et al., "Preparation of a New Crystal Form of Manganese Dioxide: λ-MnO_2," *Journal of Solid State Chemistry* 39, 142-147 (1981)

[23] D. Kim et al., “Full picture discovery for mixed-fluorine anion effects on high-voltage spinel lithium nickel manganese oxide cathodes,” *Npg Asia Mater.*, vol. 9, p. e398, Jul. 2017.

[24] G.-H. Kim, J.-H. Kim, S.-T. Myung, C. S. Yoon, and Y.-K. Sun, “Improvement of High-Voltage Cycling Behavior of Surface-Modified $Li[Ni_{1/3}Co_{1/3}Mn_{1/3}]O_2$ Cathodes by Fluorine Substitution for Li-Ion Batteries,” *J. Electrochem. Soc.*, vol. 152, no. 9, pp. A1707–A1713, Sep. 2005.

[25] P. Yue et al., “The enhanced electrochemical performance of $LiNi_{0.6}Co_{0.2}Mn_{0.2}O_2$ cathode materials by low temperature fluorine substitution,” *Electrochim. Acta*, vol. 95, no. Supplement C, pp. 112–118, 2013.

[26] J. K. Ngala, S. Alia, A. Dobley, V. M. B. Crisostomo, and S. L. Suib, "Characterization and Electrocatalytic Behavior of Layered Li_2MnO_3 and Its Acid-Treated Form," Chem. Mater., vol. 19, no. 4, pp. 229–234, 2007.